Inorg. Chem. **2006**, *45*, 10895–10904

Mononuclear Ni(III) Complexes $[Ni^{III}(L)(P(C_6H_3\text{-}3\text{-}SiMe_3\text{-}2\text{-}S)_3)]^{0/1-}$ (L = Thiolate, Selenolate, CH_2CN, Cl, PPh_3): Relevance to the Nickel Site of [NiFe] Hydrogenases

Chien-Ming Lee,[†] Ya-Lan Chuang,[†] Chao-Yi Chiang,[†] Gene-Hsiang Lee,[‡] and Wen-Feng Liaw*,[†]

Department of Chemistry, National Tsing Hua University, Hsinchu 30043, Taiwan, and Instrumentation Center, National Taiwan University, Taipei, Taiwan

Received July 26, 2006

The stable mononuclear Ni(III)–thiolate complexes $[Ni^{III}(L)(P(C_6H_3\text{-}3\text{-}SiMe_3\text{-}2\text{-}S)_3)]^-$ (L = SePh (**2**), Cl (**3**), SEt (**4**), 2-S-C_4H_3S (**5**), CH_2CN (**7**)) were isolated and characterized by UV–vis, EPR, IR, SQUID, CV, ^1H NMR, and single-crystal X-ray diffraction. The increased basicity (electronic density) of the nickel center of complexes $[Ni^{III}(L)(P(C_6H_3\text{-}3\text{-}SiMe_3\text{-}2\text{-}S)_3)]^-$ modulated by the monodentate ligand L and the substituted groups of the phenylthiolate rings promotes the stability and reactivity. In contrast to the irreversible reduction at –1.17 V (vs Cp_2Fe/Cp_2Fe^+) for complex **3**, the cyclic voltammograms of complexes $[Ni^{III}(SePh)(P(o\text{-}C_6H_4S)_3)]^-$, **2**, **4**, and **7** display reversible $Ni^{III/II}$ redox processes with $E_{1/2}$ = –1.20, –1.26, –1.32, and –1.34 V (vs Cp_2Fe/Cp_2Fe^+), respectively. Compared to complex **2** containing a phenylselenolate-coordinated ligand, complex **4** with a stronger electron-donating ethylthiolate coordinated to the Ni(III) promotes dechlorination of CH_2Cl_2 to yield complex **3** ($k_{obs} = (6.01 \pm 0.03) \times 10^{-4}$ s^{-1} for conversion of complex **4** into **3** vs $k_{obs} = (4.78 \pm 0.02) \times 10^{-5}$ s^{-1} for conversion of complex **2** into **3**). Interestingly, addition of CH_3CN into complex **3** in the presence of sodium hydride yielded the stable Ni(III)–cyanomethanide complex **7** with a Ni^{III}–CH_2CN bond distance of 2.037(3) Å. The Ni^{III}–SEt bond length of 2.273(1) Å in complex **4** is at the upper end of the 2.12–2.28 Å range for the Ni^{III}–S bond lengths of the oxidized-form [NiFe] hydrogenases. In contrast to the inertness of complexes **3** and **7** under CO atmosphere, carbon monoxide triggers the reductive elimination of the monodentate chalcogenolate ligand of complexes **2**, **4**, and **5** to produce the trigonal bipyramidal complex $[Ni^{II}(CO)(P(C_6H_3\text{-}3\text{-}SiMe_3\text{-}2\text{-}S)_3)]^-$ (**6**).

Introduction

Hydrogenases catalyze the reversible two-electron oxidation of H_2 in aerobic and anaerobic micro-organisms.[1] Two classes of hydrogenases, [Fe]-only hydrogenases ([Fe]-only H_2ases) and [NiFe] hydrogenases ([NiFe] H_2ases), have been studied widely.[1,2] The X-ray crystallographic studies of the active-site structure of [NiFe] hydrogenases isolated from *D. gigas*, *D. vulgaris*, *D. fructosovorans*, and *D. desulfuricans* ATCC27774 in combination with infrared spectroscopy have revealed an active site comprised of a hetero-bimetallic $(S_{cys})_2Ni(\mu\text{-}S_{cys})_2(\mu\text{-}X)Fe(CO)(CN)_2$ (X = O^{2-}, HO_2^-, OH^-) cluster.[3–6] The bridging ligand X was proposed to be an oxide, hydroxide, or hydro-peroxide in the oxidized state and was found to be absent in the reduced state. The coordination

* To whom correspondence should be addressed. E-mail: wfliaw@mx.nthu.edu.tw.
[†] National Tsing Hua University.
[‡] National Taiwan University.

(1) (a) Carepo, M.; Tierney, D. L.; Brondino, C. D.; Yang, T. C.; Pamplona, A.; Telser, J.; Moura, I.; Moura, J. J. G.; Hoffman, B. M. *J. Am. Chem. Soc.* **2002**, *124*, 281−286. (b) Albracht, S. P. J. *Biochim. Biophys. Acta* **1994**, *1188*, 167−204. (c) Adams, M. W. W.; Stiefel, E. I. *Curr. Opin. Chem. Biol.* **2000**, *4*, 214−220. (d) Fan, C.; Teixeira, M.; Moura, J.; Moura, I.; Huynh, B. H.; Le Gall, J.; Peck, H. D., Jr.; Hoffman, B. M. *J. Am. Chem. Soc.* **1991**, *113*, 20−24. (e) Whitehead, J. P.; Gurbiel, R. J.; Bagyinka, C.; Hoffman, B. M.; Maroney, M. J. *J. Am. Chem. Soc.* **1993**, *115*, 5629−5635.

(2) (a) Volbeda, A.; Charon, M. H.; Piras, C.; Hatchikian, E. C.; Frey, M.; Fontecilla-Camps, J. C. *Nature* **1995**, *373*, 580−587. (b) Garcin, E.; Vernede, X.; Hatchikian, E. C.; Volbeda, A.; Frey, M.; Fontecilla-Camps, J.-C. *Structure* **1999**, *7*, 557−566. (c) Happe, R. P.; Roseboom, W.; Pierik, A. J.; Albracht, S. P. J. *Nature* **1997**, *385*, 126. (d) Volbeda, A.; Garcin, E.; Piras, C.; De Lacey, A. L.; Fernandez, V. M.; Hatchikian, E. C.; Frey, M.; Fontecilla-Camps, J. C. *J. Am. Chem. Soc.* **1996**, *118*, 12989−12996. (e) Volbeda, A.; Martin, L.; Cavazza, C.; Matho, M.; Faber, B. W.; Roseboom, W.; Albracht, S. P. J.; Garcin, E.; Rousset, M.; Fontecilla-Camps, J. C. *J. Biol. Inorg. Chem.* **2005**, *10*, 239−249.

(3) (a) Higuchi, Y.; Yagi, T.; Yasuoka, N. *Structure* **1997**, *5*, 1671−1680. (b) Higuchi, Y.; Ogata, H.; Miki, K.; Yasuoka, N.; Yagi, T. *Structure* **1999**, *7*, 549−556. (c) Ogata, H.; Mizoguchi, Y.; Mizuno, N.; Miki, K.; Adachi, S.-I.; Yasuoka, N.; Yagi, T.; Yamauchi, O.; Hirota, S.; Higuchi, Y. *J. Am. Chem. Soc.* **2002**, *124*, 11628−11635. (d) Foerster, S.; Stein, M.; Brecht, M.; Ogata, H.; Higuchi, Y.; Lubitz, W. *J. Am. Chem. Soc.* **2003**, *125*, 83−93. (e) Ogata, H.; Hirota, S.; Nakahara, A.; Komori, H.; Shibata, N.; Kato, T.; Kano, K.; Higuchi, Y. *Structure* **2005**, *13*, 1635−1642.

10.1021/ic061399g CCC: $33.50
Published on Web 12/06/2006

environment about nickel in the [NiFe] H_2ases is pseudo-tetrahedral in the reduced state and pseudo-square pyramidal in the oxidized state. The nickel site has been proposed to be redox-active and changes between Ni(III) and Ni(II), while the iron site remains as Fe(II) in all spectrally defined redox states of the enzyme.[3−8] The EXAFS/EPR studies indicate that the formal oxidation state of the Ni center is paramagnetic Ni(III) in Ni−A, Ni−B, and Ni−C states.[1−9] Actually, the active form Ni−C (the paramagnetic Ni−C intermediate) of [NiFe] H_2ase was proposed to exist as the $[(S_{cys}-H)Ni^{III}-H-Fe]$ intermediates after an active state Ni−SIa (silent-active $[(S_{cys}-H)Ni^{II}(S_{cys})_3]$) is passed. Ni−C is believed to be an intermediate in the catalytic cycle.[1−9] Upon illumination, the Ni−C state is transformed into a fourth paramagnetic Ni−L state. These conversions are considered to correspond to photodissociation of proton species from the [Ni−Fe] center.[3d] Interestingly, the recent X-ray crystal structures of CO-inhibited forms and single-crystal EPR studies of the reduced active site of [NiFe] H_{2ase} isolated from *D. vulgaris* Miyazaki F implicate that the Ni−C intermediate is a formal Ni(III) oxidation state with a hydride (H^-) bridging between the Ni and the Fe atoms and the sulfur atom of Cys 546 hydrogenated for the catalytic reaction of the enzyme.[3c] Meanwhile, the Ni−C state subsequently transformed into Ni−CO forms under an exogenous CO atmosphere.[3c]

Several mononuclear nickel−thiolate complexes have been synthesized to afford the information about the structure of the Ni active state of [NiFe] H_2ase.[10] An electrochemical study provided evidence for such a Ni(III)−H species generated by one-electron reduction of a nickel(II) macrocyclic complex accompanied by protonation.[11] The mononuclear complex $[Ni(psnet)]^+$ of known structure can stoichiometrically evolve H_2 from protic sources.[10c,d] The reaction pathways were proposed as involving steps of protic oxidative addition to Ni(I) to generate $Ni^{III}-H^-$, and electron transfer to Ni(III) accompanied by protonation of bound hydride or the bimolecular reaction ($2Ni^{III}-H^- \rightarrow 2Ni^{II} + H_2$) to yield H_2.[10c,d] Complex $Ni^{II}(Bm^{Me})_2$ (Bm^{Me} = bis(2-mercapto-1-methylimidazolyl)borate) with a $[NiS_4H_2]$ core and the presence of Ni···H − B interaction may provide a structural model of the nickel site of [NiFe] H_2ase.[12] Recently, Tatsumi and co-workers reported the isolation of dithiolato-bridged $[Fe(CO)_2(CN)_2(\mu\text{-}SCH_2CH_2CH_2S)Ni(S_2\text{-}CNR_2)]^-$ (R = Et; $R_2 = -(CH_2)_5-$) complexes, displaying the closely structural feature of the active site of reduced form [NiFe] H_2ase.[13]

In the previous study of complexes $[Ni^{II}(L)(P\text{-}(o\text{-}C_6H_4S)_2\text{-}(o\text{-}C_6H_4SH))]^{0/1-}$ (L = PPh_3, SePh, SPh, and Cl), the interaction between the pendent thiol proton and both the nickel and sulfur atoms (a combination of intramolecular [Ni−S···H−S] and [Ni···H−S] interactions) was demonstrated.[14] The extent of interactions between the pendent thiol proton and both the nickel and sulfur atoms in complexes $[Ni^{II}(L)(P\text{-}(o\text{-}C_6H_4S)_2(o\text{-}C_6H_4SH))]^{0/1-}$ was modulated by the monodentate ligand L. Examples of thiolate coordination to nickel(III) and the spectroscopic signals of nickel(III)−thiolate complexes are of much interest, particularly in catalytically active site construction (Ni−A/Ni−B states) of the nickel active site of [NiFe] hydrogenases. By application of oxidation, dechlorination, and stepwise ligand exchange, we have prepared $[PPN][Ni^{III}(L)(P(C_6H_3\text{-}3\text{-}Si-Me_3\text{-}2\text{-}S)_3)]$ (L = SePh (**2**), Cl (**3**), SEt (**4**), 2-S−C_4H_3S (**5**), CH_2CN (**7**)), characterized by UV−vis, EPR, IR, CV, SQUID, and X-ray crystallography. This study further provides the evidence that the different monodentate ligands $[SePh]^-$, $[Cl]^-$, $[SEt]^-$, $[2\text{-}S-C_4H_3S]^-$, $[CH_2CN]^-$, and PPh_3, rendering the $[Ni^{III}\text{-}(P(C_6H_3\text{-}3\text{-}Si-Me_3\text{-}2\text{-}S)_3)]$ motif in different electronic environments, induce different stability and reactivity.

Results and Discussion

Reaction of Complex $[Ni^{II}(SePh)(P(C_6H_3\text{-}3\text{-}SiMe_3\text{-}2\text{-}S)_2\text{-}(C_6H_3\text{-}3\text{-}SiMe_3\text{-}2\text{-}SH))]^-$ (1) with Dioxygen. In contrast to $[Ni(SePh)(P(o\text{-}C_6H_4S)_2(o\text{-}C_6H_4-SH))]^-$,[14a] which is slightly soluble in THF solution, the ligand-modified analogue $[Ni(SePh)(P(C_6H_3\text{-}3\text{-}SiMe_3\text{-}2\text{-}S)_2(C_6H_3\text{-}3\text{-}SiMe_3\text{-}2\text{-}SH))]^-$ (**1**) shows significant solubility. Reaction of $[Ni(CO)(SePh)_3]^-$ and $P(C_6H_3\text{-}3\text{-}SiMe_3\text{-}2\text{-}SH)_3$ in a 1:1 stoichiometry in THF led to the formation of complex **1** isolated as a dark red-brown solid.[14] Complex **1** reveals the ν_{SH} stretching band at 2250 cm^{-1} (KBr) in IR spectroscopy and the chemical shift of the SH group at δ 8.59 (d) ppm (C_4D_8O) in ^1H NMR spectroscopy. These results show the existence of intramolecular [Ni−S···H−S] interaction (or a combination of intramolecular [Ni−S···H−S] and [Ni···H−S] interactions) as observed in complex $[Ni(SePh)(P(o\text{-}C_6H_4S)_2(o\text{-}C_6H_4-$

(4) (a) Rousset, M.; Montet, Y.; Guigliarelli, B.; Forget, A.; Asso, M.; Bertrand, P.; Fontecilla-Camps, J. C.; Hatchikian, E. C. *Proc. Natl. Acad. Sci. U.S.A.* **1998**, *95*, 11625−11630. (b) Tye, J. W.; Hall, M. B.; Darensbourg, M. Y. *Proc. Natl. Acad. Sci. U.S.A.* **2005**, *102*, 16911−16912.

(5) Matias, P. M.; Soares, C. M.; Saraiva, L. M.; Coelho, R.; Morais, J.; Le Gall, J.; Carrondo, M. A. *J. Biol. Inorg. Chem.* **2001**, *6*, 63−81.

(6) (a) De Lacey, A. L.; Hatchikian, E. C.; Volbeda, A.; Frey, M.; Fontecilla-Camps, J. C.; Fernandez, V. M. *J. Am. Chem. Soc.* **1997**, *119*, 7181−7189. (b) Maroney, M. J.; Davidson, G.; Allan, C. B.; Figlar, J. *Struct. Bond.* **1998**, *92*, 1−65. (c) Bagley, K. A.; Duin, E. C.; Roseboom, W.; Albracht, S. P. J.; Woodruff, W. H. *Biochemistry* **1995**, *34*, 5527−5535. (d) Coremans, J. M. C. C.; van der Zwaan, G. W.; Albracht, S. P. J. *Biochim. Biophys. Acta* **1992**, *1119*, 157−168. (e) Stein, M.; Lubitz, W. *Curr. Opin. Chem. Biol.* **2002**, *6*, 243−249.

(7) Niu, S.; Thomson, L. M.; Hall, M. B. *J. Am. Chem. Soc.* **1999**, *121*, 4000−4007.

(8) De Gioia, L.; Fantucci, P.; Guigliarelli, B.; Bertrand, P. *Inorg. Chem.* **1999**, *38*, 2658−2662.

(9) Foerster, S.; van Gastel, M.; Brecht, M.; Lubitz, W. *J. Biol. Inorg. Chem.* **2005**, *10*, 51−62.

(10) (a) Darensbourg, M. Y.; Lyon, E. J.; Smee, J. *Coord. Chem. Rev.* **2000**, *206*, 533−561. (b) Allan, C. B.; Davidson, G.; Choudhury, S. B.; Gu, Z.; Bose, K.; Day, R. O.; Maroney, M. J. *Inorg. Chem.* **1998**, *37*, 4166−4167. (c) James, T. L.; Cai, L.; Mutterties, M. C.; Holm, R. H. *Inorg. Chem.* **1996**, *35*, 4148−4161. (d) Cha, M.; Shoner, S. C.; Kovacs, J. A. *Inorg. Chem.* **1993**, *32*, 1860−1863. (e) Nguyen, D. H.; Hsu, H.-F.; Millar, M.; Koch, S. A.; Achim, C.; Bominaar, E. L.; Münck, E. *J. Am. Chem. Soc.* **1996**, *118*, 8963−8964. (f) Bouwman, E.; Reedijk, J. *Coord. Chem. Rev.* **2005**, *249*, 1555−1581.

(11) Efros, L. L.; Thorp, H. H.; Brudvig, G. W.; Crabtree, R. H. *Inorg. Chem.* **1992**, *31*, 1722−1724.

(12) Alvarez, H. M.; Krawiec, M.; Donovan-Merkert, B. T.; Fouzi, M.; Rabinovich, D. *Inorg. Chem.* **2001**, *40*, 5736−5737.

(13) Li, Z.; Ohki, Y.; Tatsumi, K. *J. Am. Chem. Soc.* **2005**, *127*, 8950−8951.

(14) (a) Lee, C.-M.; Chen, C.-H.; Ke, S.-C.; Lee, G.-H.; Liaw, W.-F. *J. Am. Chem. Soc.* **2004**, *126*, 8406−8412. (b) Chen, C.-H.; Lee, G.-H.; Liaw, W.-F. *Inorg. Chem.* **2006**, *45*, 2307−2316.

Scheme 1

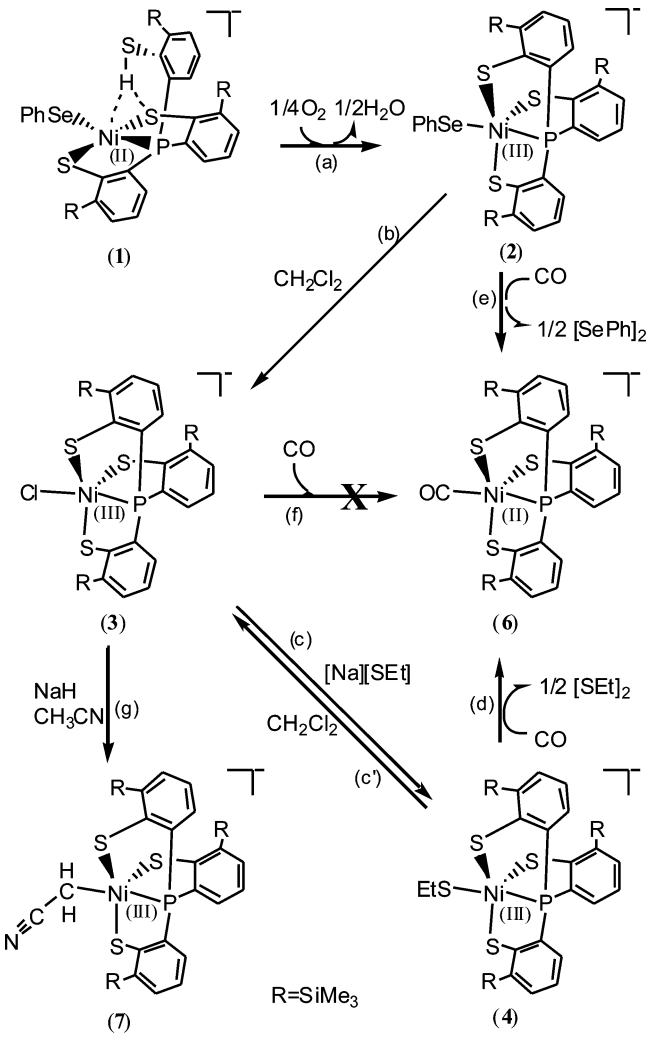

SH))]$^-$.[14] The H/D exchange reaction occurred between complex **1** and D_2O (excess) in THF solution at room temperature for 24 h to yield [Ni(SePh)(P(C$_6$H$_3$-3-SiMe$_3$-2-S)$_2$(C$_6$H$_3$-3-SiMe$_3$-2-SD))]$^-$ (**1-D**) with a ν_{SD} stretching band at 1665 (br) cm^{-1} (KBr). A ^{2}H NMR resonance that appeared as a broad peak at δ 8.43 ppm (THF) also supports the formation of complex **1-D** (using natural abundance of D in C_4H_8O as internal standard, δ 1.73 and 3.58 ppm).[14]

Upon injection of 1 equiv of dry O_2 into a THF solution of 4 equiv of complex **1**, a pronounced color change from red-brown to dark green occurs at room temperature. Single-crystal X-ray diffraction study, UV−vis, and ^{1}H NMR spectrum confirmed the complete formation of the mononuclear [PPN][Ni^{III}(SePh)(P(C$_6$H$_3$-3-SiMe$_3$-2-S)$_3$)] (**2**) accompanied by byproduct H_2O (Scheme 1a).[14a] To unambiguously prove the formation of H_2O, the THF solution of complex **1-D** was treated with dry O_2 at ambient temperature. A ^{2}H NMR resonance at δ 8.43 ppm due to SD of **1-D** in C_4H_8O disappeared along with the formation of the byproduct D_2O with resonance at δ 2.02 ppm in C_4H_8O (Supporting Information Figure S1).[14a] The ^{1}H NMR spectrum of complex **2** at 298 K exhibits the paramagnetic chemical shifts that appear at δ −4.25 (br), 3.03 (br), 6.50 (br), 10.15 (br), 11.01 (br), 14.77 (br) (SePh, *o*-C$_6$H$_3$S); 2.13 (s), 2.24 (s) (SiMe$_3$) ppm (in CD_3CN). Reaction of complex **1** and O_2 in THF−CH_3CN (1:1 volume ratio) was also monitored by UV−vis at ambient temperature. The increase of intensity of absorption bands 590, 772, and 954 nm with no isosbestic points indicates the existence of intermediates during the oxidative transformation of complex **1** to **2** in the first 30 min (Supporting Information Figure S2(a)). Then the intensity of absorptions at 590 and 954 nm (complex **2**) continuously increases while the intensity of absorption at 772 nm decreases with two isosbestic points (Supporting Information Figure S2(b)). Thus, this spectroscopic evidence may further support the mechanism proposed in the previous report to explain the formation of [Ni^{III}(SePh)(P(*o*-C$_6$H$_4$S)$_3$)]$^-$ via O_2 oxidation of complex [Ni^{II}(SePh)(P(*o*-C$_6$H$_4$S)$_2$(*o*-C$_6$H$_4$-SH))]$^-$.[14a] However, the intermediate cannot be unambiguously characterized at this moment. In contrast to [Ni^{III}-(SePh)(P(*o*-C$_6$H$_4$S)$_3$)]$^-$,[14a] which is unstable in THF solution, the ligand-modified analogue complex **2** displays the thermal stability in THF solution. Presumably, the more electron-rich functionalities of Ni(III) center (the strongly σ-donating $SiMe_3$ group acting as an effective promoter of Ni(III) metal π-donating ability)[15] are responsible for the stabilization of the Ni(III) state to prevent reduction of the Ni(III) by the monodentate phenylselenolate ligand.

Preparations of Complexes [PPN][Ni^{III}(L)(P(C$_6$H$_3$-3-Si−Me$_3$-2-S)$_3$)] (L = Cl (3), SEt (4), 2-S−C$_4$H$_3$S (5)). As shown in Scheme 1b, addition of CH_2Cl_2 to complex **2** in the absence of dioxygen produced [PPN][Ni^{III}(Cl)(P(C$_6$H$_3$-3-Si−Me$_3$-2-S)$_3$)] (**3**). The ^{1}H NMR spectrum of the crystalline product obtained from diffusion of diethyl ether into a CH_2Cl_2 solution of complex **2** at ambient temperature for 1 week exhibits three broadening proton resonances at δ −6.47, 9.59, and 16.20 ppm (CD_3CN), also implicating the formation of complex **3**. Upon introduction of complex **2** into CH_2Cl_2 and monitoring by UV−vis, the UV−vis spectrum showing four intense absorptions (430, 620, 760, and 990 nm) and three isosbestic points suggest a straightforward conversion of complex **2** into complex **3** occurred at ambient temperature (Supporting Information Figure S3). To our knowledge, ligand-based reactivity of transition-metal thiolates is well-documented.[16] The formation of nickel−thiolate aggregates adopting thiolate or methylene group as linkages derived from CH_2Cl_2 was reported by Schröder and co-workers.[17] In particular, Karlin and co-workers reported that copper(I) complexes with tertiary amine and pyridyl ligands triggered the dechlorination of CH_2Cl_2, $CHCl_3$, and benzyl chloride to yield Cu^{II}−Cl complexes.[18]

(15) (a) Macgregor, S. A.; Lu, Z.; Eisenstein, O.; Crabtree, R. H. *Inorg. Chem.* **1994**, *33*, 3616−3618. (b) Saint-Joly, C.; Mari, A.; Dartiguenave, M.; Dartiguenave, Y.; Galy, J. *Inorg. Chem.* **1980**, *19*, 2403−2410. (c) Liaw, W.-F.; Horng, Y.-C.; Ou, D.-S.; Chiang, C.-Y.; Lee, G.-H.; Peng, S.-M. *J. Am. Chem. Soc.* **1997**, *119*, 9299−9300. (d) Liaw, W.-F.; Chen, C.-H.; Lee, C.-M.; Lee, G.-H.; Peng, S.-M. *J. Chem. Soc., Dalton Trans.* **2001**, 138−143.

(16) Grapperhaus, C. A.; Poturovic, S.; Mashuta, M. S. *Inorg. Chem.* **2002**, *41*, 4309−4311.

(17) Wang, Q.; Marr, A. C.; Blake, A. J.; Wilson, C.; Schröder, M. *Chem. Commun.* **2003**, 2776−2777 and references therein.

(18) Lucchese, B.; Humphreys, K. J.; Lee, D.-H.; Incarvito, C. D.; Sommer, R. D.; Rheingold, A. L.; Karlin, K. D. *Inorg. Chem.* **2004**, *43*, 5987−5998.

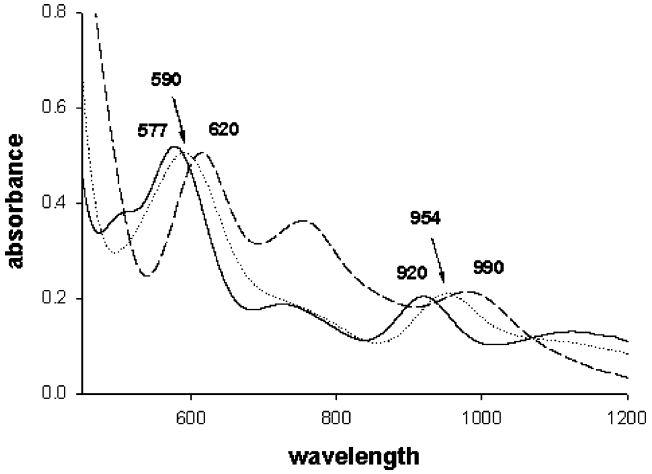

Figure 1. UV−vis spectra (in CH_3CN) of complexes **2** (dotted line ···), **3** (dashed line ---), and **4** (solid line −), respectively. Only two intense absorptions were labeled for comparison.

To further examine the effect of electronic modulations of the monodentate ligand L on the stability of $[Ni^{III}(L)(P(C_6H_3\text{-}3\text{-}SiMe_3\text{-}2\text{-}S)_3)]^-$ complexes, complex [PPN][Ni(SEt)($P(C_6H_3$-3-$SiMe_3$-2-$S)_3$)] (**4**) containing coordinated ethylthiolate was synthesized by adopting complex **3** serving as a precursor. When a $CH_3CN-THF$ (1:3 v/v) solution of complex **3** and [Na][SEt] were stirred under N_2 at ambient temperature, a rapid reaction ensues over the course of 30 min to give the dark-green [PPN][Ni(SEt)($P(C_6H_3$-3-$SiMe_3$-2-$S)_3$)] (**4**) (60% yield) after removal of insoluble NaCl and recrystallization with $CH_3CN-THF$/diethyl ether (Scheme 1c). It is noticed that the metathesis reaction of complex **3** and [Na][SEt] prefers to follow the dropwise addition of complex **3** (in $CH_3CN-THF$) to CH_3CN solution of [Na][SEt]. If the sequence of addition was reversed, complex **4** was isolated in low yield.[19] Complex **4** is soluble in $CH_3CN-THF$ (1:3 v/v ratio) and shows the dark green color in solution. A single-crystal X-ray diffraction study confirmed the formation of complex **4**, the first structurally characterized Ni(III)−alkylthiolate species. In comparison with complexes **2** and **3** dominated by two intense absorption bands at (590, 954) nm and (620, 990) nm, respectively, the electronic spectrum of complex **4** coordinated by the more electron-donating ethylthiolate displays blue shifts to (577, 920) nm (Figure 1). Complex **4** exhibits a diagnostic ^1H NMR spectrum with phenyl and ethyl proton resonances well-removed from the diamagnetic region. The proton resonances (δ 40.67 (br), 3.17 (br) ppm and 14.97 (br), 10.27 (br), −3.05 (br) ppm) were assigned to $[SEt]^-$ and $[P(C_6H_3$-3-$SiMe_3$-2-$S)_3]^{3-}$ ligands, respectively. This result is consistent with the central Ni^{III} possessing a d^7 electronic configuration in a trigonal bipyramidal ligand field.[14a] In a similar fashion, reaction of complex **3** and [Na][2-S−C_4H_3S] in $THF-CH_3CN$ solution also led to the formation of [PPN][Ni(2-S−C_4H_3S)($P(C_6H_3$-3-$SiMe_3$-2-$S)_3$)] (**5**) (yield 60%) (Supporting Information Figure S4).

The influence of the coordinated $[SEt]^-$ ligand on the chemical reactivity of complex **4** was also investigated. As shown in Scheme 1c, dissolving complex **4** in CH_2Cl_2 at room temperature also led to the formation of complex **3**. This result confirms that complexes **2** and **4** containing Ni(III)−SePh and Ni(III)−SEt bonds, respectively, serve as a nucleophile for dechlorination of CH_2Cl_2. The dechlorination reaction between complex **2** (or complex **4**) and CH_2Cl_2 was followed by a UV−vis spectrum with the characteristic absorption 760 nm of complex **3** at 23 (±) °C. The conversion of complex **4** to **3** is faster than that of complex **2** to **3** in excess CH_2Cl_2 ($k_{obs} = (6.01 \pm 3) \times 10^{-4}$ s^{-1} for conversion of complex **4** into **3** and $k_{obs} = (4.78 \pm 0.02) \times 10^{-5}$ s^{-1} for conversion of complex **2** into **3**; Supporting Information Figure S5).

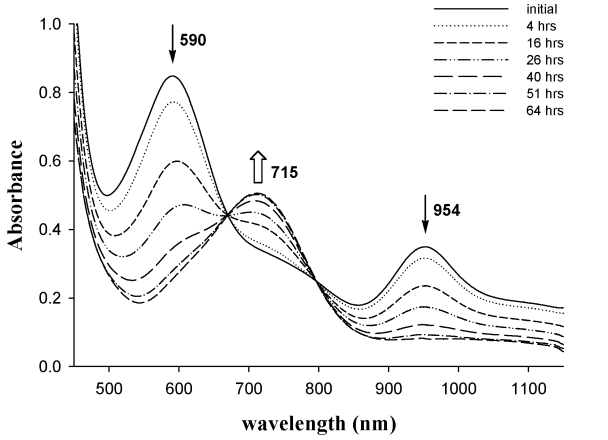

Figure 2. Reaction between complex **2** and CO in CH_3CN was monitored by UV−vis spectra. The measured intervals between two curves are shown in the diagram.

Reductive Elimination of Ni(III)−SePh and Ni(III)−SEt Bonds under CO Atmosphere. When a $THF-CH_3CN$ (3:1 v/v) solution of complex **2** (or complexes **4** and **5**) (0.03 mmol) was treated with CO (1 atm) at ambient temperature for 80 h, complex **2** (or complexes **4** and **5**) completely transformed into complex [PPN][Ni^{II}(CO)($P(C_6H_3$-3-$SiMe_3$-2-$S)_3$)] (**6**), as monitored by UV−vis (Figure 2) and IR with a ν_{CO} stretching band (2033 cm^{-1}, KBr), accompanied by formation of diphenyl diselenide (diethyl disulfide, di(2-thienyl) disulfide) identified by ^1H NMR spectrum (Scheme 1d,e). Obviously, CO molecule triggers the reductive elimination of the coordinated phenylselenolate of complex **2** (or ethylthiolate of complex **4,** 2-thienylthiolate of complex **5**) to yield Ni(II)−CO complex **6** (Supporting Information Figure S6) and byproduct $(PhSe)_2$ (or $(SEt)_2$/$(2\text{-}S-C_4H_3S)_2$), relevant to the observation that Ni−C state was converted into the Ni−L form under illumination which subsequently transformed into Ni−CO state under exogenous CO condition in [NiFe] hydrogenase isolated from *D. vulgaris* Miyazaki F.[3c,d] It is presumed that the σ-/π-electron-donating nature of the coordinated thiolates/selenolate converts Ni(II), a weaker π-donor, into a strong π-donor and favors Ni−CO bonding.[15] Compared to complex **2** (Scheme 1e), the easier reductive elimination of the coordinated ethylthiolate of complex **4** under CO atmosphere accompanied by the formation of Ni(II)−CO complex **6** is presumably ascribed to the more electron-rich Ni center of complex **4** which promotes the coordination of CO to Ni-

(19) Rosenfield, S. G.; Armstrong, W. H.; Mascharak, P. K. *Inorg. Chem.* **1986**, *25*, 3014−3018.

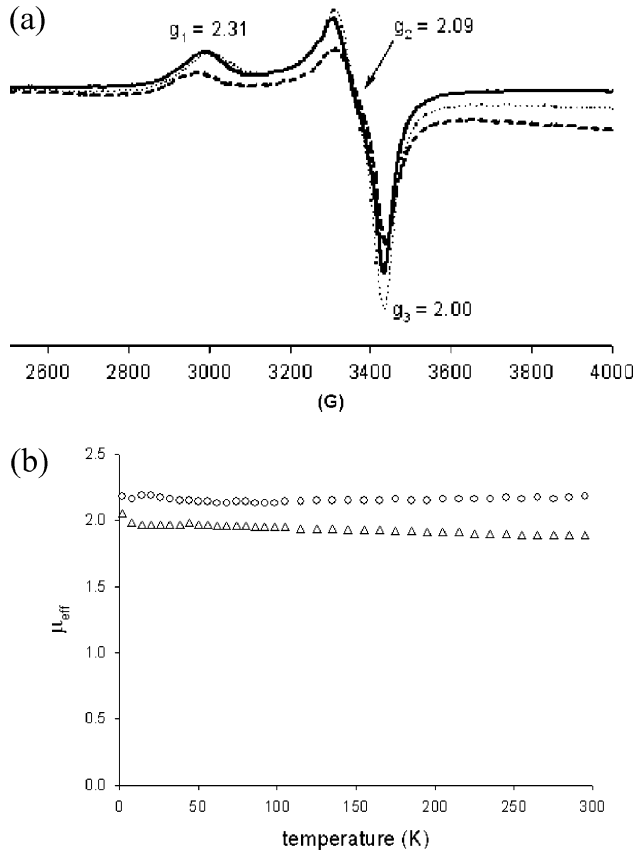

Figure 3. (a) EPR spectra of complex **2** (dashed line ---), complex **3** (dotted line ···), and complex **4** (solid line —) at 77 K. (b) Plots of μ_{eff} vs T for complexes **2** (triangle up △△△) and **3** (circle ○○○).

Table 1. Half-wave Potentials ($E_{1/2}$) (vs Cp_2Fe/Cp_2Fe^+) for Complexes [Ni^{III}(SePh)(P(*o*-C$_6$H$_4$S)$_3$)]$^-$, **2**, **3**, **4**, and **7** in CH_3CN (Complex **9** in CH_2Cl_2) at 100 mV/s Scan Rate

compound	$E_{1/2}$ (V)	E_{red} (V)
[Ni^{III}(SePh)(P(*o*-C$_6$H$_4$S)$_3$)]$^-$	−1.20	
2	−1.26	
3		−1.17
4	−1.32	
7	−1.34	
9	−0.83	

(III) center and the subsequent reductive elimination of ethylthiolate (Supporting Information Figure S7). However, upon CO bubbled into a THF−CH_3CN (1:1 v/v) solution of complex **3**, no ν_{CO} stretching band in the IR spectrum and changes of absorption bands (430, 620, 760, and 990 nm) in the UV−vis spectrum were observed (Scheme 1f). This result implies that the Ni(III)−Cl bond of complex **3** is resistant to undergoing reductive elimination, in contrast to the Ni(III)−SePh and Ni(III)−SEt bonds of complexes **2** and **4**, respectively. The Ni(II)−CO of complex **6** is not photolabile. THF solution of complex **6** is stable under photolysis (λ = 365 nm) for 7 h at ambient temperature.

The preferred geometry of complex **6** is a distorted trigonal bipyramidal with CO occupying an axial position (Supporting Information Figure S6). This is presumably because the chelating [P(C$_6$H$_3$-3-SiMe$_3$-2-S)$_3$]$^{3-}$ has to occupy the equatorial sites and one of the axial sites.[15a] CO bonded to Ni(II) in a square planar geometry has been isolated and characterized.[15c,d] In addition, the computation has demonstrated that the most favorable geometries of CO binding to Ni(II) are trigonal bipyramidal with CO occupying equatorial or square pyramidal with CO occupying axial.[15a] Compared to complex [Ni(CO)Cl$_2$(PMe$_3$)$_2$] (ν_{CO}: 2005 cm^{-1} and Ni−CO bond distance of 1.730(2) Å),[15a,b] the CO stretching frequency of 2033 cm^{-1} (CH_3CN) is higher and the Ni−CO bond length of 1.800(6) Å is longer in complex **6**.

Synthesis of Ni(III)−Cyanomethanide Complex. The unprecedented nickel(III)−thiolate complex containing C-bonded cyanomethanide [PPN][Ni(CH_2CN)(P(C$_6$H$_3$-3-SiMe$_3$-2-S)$_3$)] (**7**) was isolated (yield 65%) from reaction of complex **3** and CH_3CN in the presence of NaH at ambient temperature (Scheme 1g).[20] The formation of complex **7** is probably initiated by an anionic deprotonation of CH_3CN followed by a nucleophilic attack by the [CH_2CN]$^-$ carbanion on Ni and the precipitation of NaCl.[20a] In comparisons of complexes **2**, **3**, and **4** dominated by two intense absorption bands at (590, 954), (620, 990), and (577, 920) nm in UV−vis spectra, respectively, the electronic spectrum of complex **7** coordinated by −CH_2CN displays blue shifts to 543 and 925 nm. Carbon monoxide did not trigger the reductive elimination of Ni(III)−CH_2CN bond, even exposing the CH_3CN solution of complex **7** under 1 atm of CO at ambient temperature for 4 days.[20a] Obviously, the reactivity of complexes [Ni^{III}(L)-(P(C$_6$H$_3$-3-SiMe$_3$-2-S)$_3$)]$^-$ may be tailored by ligand L. To prove that the Ni(III) complexes containing the monodentate chalcogenolate ligand undergo reductive elimination of dialkyl dichalcogenides yielding Ni^{II}−CO complex **6** under CO atmosphere, we repeated the reaction of the neutral [Ni^{III}-(PPh$_3$)(P(C$_6$H$_3$-3-SiMe$_3$-2-S)$_3$)] (**9**), synthesized from oxygen oxidation of complex [Ni^{II}(PPh$_3$)(P(C$_6$H$_3$-3-SiMe$_3$-2-S)$_2$-(C$_6$H$_3$-3-SiMe$_3$-2-SH))]$^-$ (**8**),[14b] and CO (1 atm). On the basis of IR ν_{CO} and UV−vis spectra, no Ni(II)−CO complex **6** was generated after the reaction solution of complex **9** was stirred under a CO atmosphere in THF for 4 days.

EPR and Effective Magnetic Moment. The EPR spectra of complexes **2**, **3**, and **4** are identical at 77 K and exhibit rhombicity with principal g values of 2.31, 2.09, and 2.0 (Figure 3a) (g = 2.345, 2.093, and 1.99 for complex **7**). The g values (g = 2.31, 2.09, and 2.0 for complexes **2**, **3**, and **4**) much higher than the free electron g value 2.0023 implicated a large orbital contribution, and the unpaired electron is primarily associated with the nickel ion.[14a] The effective magnetic moment in solid state by a SQUID magnetometer was 1.8 and 2.1 μ_B for complexes **2** and **3**, respectively (Figure 3b), consistent with total spin value (S_T) of $^1/_2$.[14a]

Electrochemistry. Half-wave potentials ($E_{1/2}$) of complexes [Ni^{III}(SePh)(P(*o*-C$_6$H$_4$S)$_3$)]$^-$, **2**, **3**, **4**, and **7** (2.0 mM) were measured in CH_3CN with 0.1 M [*n*-Bu$_4$N][PF$_6$] as supporting electrolyte at room temperature (scan rate 100 mV/s) and listed in Table 1. In comparisons of complexes

(20) (a) Alburquerque, P. R.; Pinhas, A. R.; Bauer, J. A. K. *Inorg. Chim. Acta* **2000**, *298*, 239−244. (b) Tanaka, K.; Kushi, Y.; Tsuge, K.; Toyohara, K.; Nishioka, T.; Isobe, K. *Inorg. Chem.* **1998**, *37*, 120−126. (c) Schebler, P. J.; Mandimutsira, B. S.; Riordan, C. G.; Liable-Sands, L. M.; Incarvito, C. D.; Rheingold, A. L. *J. Am. Chem. Soc.* **2001**, *123*, 331−332. (d) Schenker, R.; Mock, M. T.; Kieber-Emmons, M. T.; Riordan, C. G.; Brunold, T. C. *Inorg. Chem.* **2005**, *44*, 3605−3617.

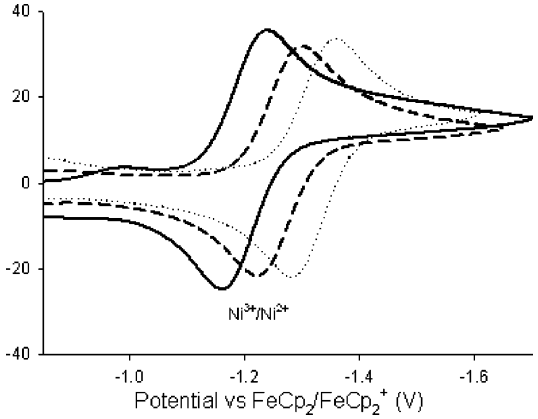

Figure 4. Cyclic voltammograms of $[Ni(SePh)(P(o\text{-}C_6H_4S)_3)]^-$ (solid line —), complex **2** (dashed line ---), and complex **4** (dotted line ···) (conditions: CH_3CN, scan rate 0.1 V/s, room temperature, and referenced to ferrocinium/ferrocene).

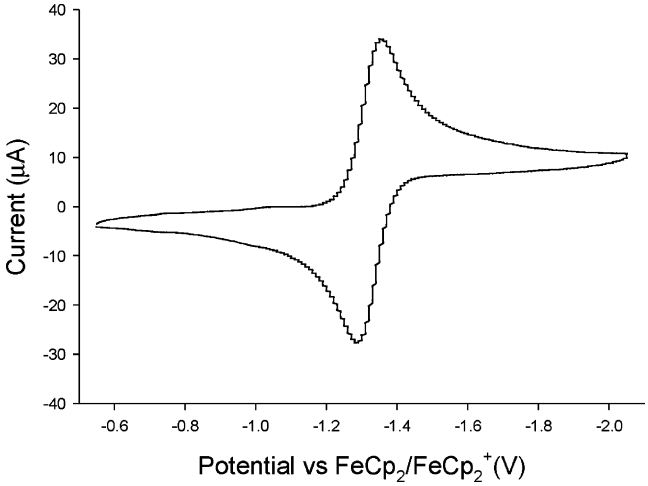

Figure 5. Cyclic voltammogram of complex **7** (conditions: CH_3CN, scan rate 0.1 V/s, room temperature, and referenced to ferrocinium/ferrocene).

$[Ni^{III}(SePh)(P(o\text{-}C_6H_4S)_3)]^-$ and **2**, the induction of trimethylsilyl substituents in the meta positions of the phenyl rings causes the $E_{1/2}$ of complex **2** to shift more negative values ($\Delta E_{1/2} = 0.06$ V; $E_{1/2} = -1.20$ V for complex $[Ni^{III}(SePh)(P(o\text{-}C_6H_4S)_3)]^-$ (vs Cp_2Fe/Cp_2Fe^+)), as shown in Figure 4. Similar effects are observed for complexes **2** and **4**. Complex **4** with a coordinated $[SEt]^-$ ligand reveals one reversible $Ni^{III/II}$ redox process at -1.32 V ($E_{1/2}$), as compared to -1.26 V ($E_{1/2}$) for complex **2** (vs Cp_2Fe/Cp_2Fe^+, Figure 4). In comparisons of complexes **2** and **4**, the more positive redox potential of Ni center in complex **2** presumably was caused by the weaker electron-donating ability of the coordinated $[SePh]^-$ ligand compared to $[SEt]^-$. Complex **9** with a coordinated PPh_3 revealing one reversible $Ni^{III/II}$ redox process at -0.83 V ($E_{1/2}$) (vs Cp_2Fe/Cp_2Fe^+) further corroborates this rationalization (Table 1 and Supporting Information Figure S8). In contrast to complexes **2** and **4** displaying a reversible Ni(III)−Ni(II) process, the cyclic voltammogram of complex **3** with a coordinated chloride ligand displays an irreversible reduction at -1.17 V (vs Cp_2Fe/Cp_2Fe^+, Supporting Information Figure S9). Although carbon monoxide did not promote the reductive elimination of Ni(III)−CH_2CN bond of complex **7**, electrochemistry of complex **7** also reveals one reversible redox process at -1.34 V (vs Cp_2Fe/Cp_2Fe^+), as shown in Figure 5.

Structures. The X-ray single-crystal structures of complexes **2**, **3**, **4**, and **7** are displayed in Figures 6, 7, 8, and 9, respectively, and selected bond distances and angles are presented in the figure captions. Complexes **2**−**4** and **7** are isostructural mononuclear Ni(III)−thiolate complexes. The strain effect of the chelating ligand ($[P(C_6H_3\text{-}3\text{-}SiMe_3\text{-}2\text{-}S)_3]^{3-}$) in the coordination sphere of complexes **2**−**4** and **7** explains the geometry of Ni is a distorted trigonal bipyramidal with three thiolates locating equatorial positions and the phosphorus occupying an axial position trans to $[SePh]^-$ in **2**, $[Cl]^-$ in **3**, $[SEt]^-$ in **4**, and $[CH_2CN]^-$ in **7**. The Ni metal was displaced from the mean three sulfur-atoms plane toward $[SePh]^-$, $[Cl]^-$, and $[SEt]^-$ ligands (0.1344(11) Å for **2**, 0.1446(8) Å for **3**, and 0.1353(14) Å for **4**), respectively. The average Ni−S bond lengths (bond lengths between the sulfur of chelating $[P(C_6H_3\text{-}3\text{-}SiMe_3\text{-}2\text{-}S)_3]^{3-}$ ligand and Ni^{III})

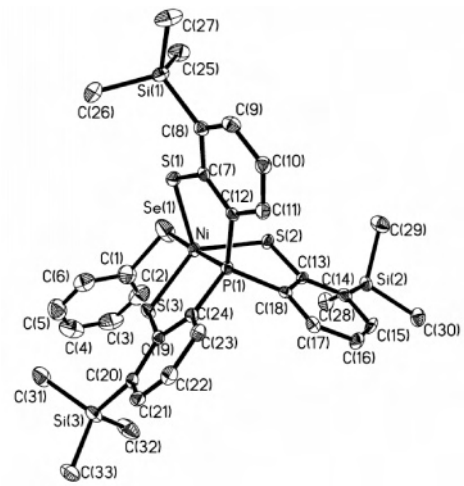

Figure 6. ORTEP drawing and labeling scheme of $[Ni^{III}(SePh)(P(C_6H_3\text{-}3\text{-}SiMe_3\text{-}2\text{-}S)_3)]^-$ (**2**) anion with thermal ellipsoids drawn at 50% probability. Selected bond distances (Å) and angles (deg): Ni−Se(1) 2.3473(8); Ni−S(1) 2.2853(12); Ni−S(2) 2.2927(12); Ni−S(3) 2.2122(12); Ni−P(1) 2.1318(12); S(1)−Ni−S(2) 106.58(5); S(1)−Ni−S(3) 119.39(5); S(2)−Ni−S(3) 132.94(5); S(1)−Ni−Se(1) 93.67(4); S(2)−Ni−Se(1) 91.75(4); S(3)−Ni−Se(1) 94.72(4); P(1)−Ni−Se(1)176.55(4); P(1)−Ni−S(1) 87.19(4); P(1)−Ni−S(2) 84.80(4); P(1)−Ni−S(3) 87.76(4).

in complexes **2**, **3**, and **4** do not show dramatic differences (2.263(1) Å for **2**, 2.258(1) Å for **3**, 2.253 (1) Å for **4,** and 2.254(1) Å for **7**). Compared to $[Ni^{III}(SePh)(P(o\text{-}C_6H_4S)_3)]^-$,[14a] the mean Ni−S bond lengths (bond lengths between the sulfur of chelating $[P(o\text{-}C_6H_4S)_3]^{3-}$ ligand and Ni^{III}) have increased by 0.014 Å and the Ni^{III}−Se bond distance has decreased by 0.024 Å in complexes **2**. The Ni^{III}−S(4) bond length of 2.273(1) Å (the distance between the monodentate ethylthiolate and Ni^{III}) in complex **4**, comparable to the Ni^{III}−S(4) bond length of 2.2554(9) Å in complex **5** (Supporting Information Figure S4), is shorter than the average Ni^{II}−S bond length of 2.281(1) Å in $[Ni(S\text{-}p\text{-}C_6H_4Cl)_4]$.[2−19] It is noticed that the Ni^{III}−C(28) (CH_2CN) bond distance of 2.037(3) Å in complex **7** is longer than the Ni^{II}−C bond lengths of 1.94(2), 1.921(8), and 1.918(5) Å observed in complexes $[Ni(NS_3{}^{iPr})Me][BPh_4]$,[21] [(2.2′-bipyridine)Ni-$(O(CH_2)_3CH_2)$],[22] and [bis(pyridine)Ni$(CH_3)_2$],[23] respectively.

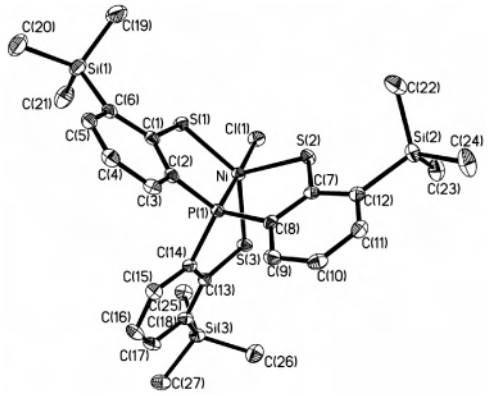

Figure 7. ORTEP drawing and labeling scheme of [Ni^{III}(Cl)(P(C$_6$H$_3$-3-SiMe$_3$-2-S)$_3$)]$^-$ (**3**) anion with thermal ellipsoids drawn at 50% probability. Selected bond distances (Å) and angles (deg): Ni−Cl(1) 2.2338(5); Ni−S(1) 2.2191(6); Ni−S(2) 2.2673(6); Ni−S(3) 2.2867(6); Ni−P(1) 2.1203(6); S(1)−Ni−S(2) 115.09(2); S(1)−Ni−S(3) 136.19(2); S(2)−Ni−S(3) 107.44(2); S(1)−Ni−Cl(1) 91.25(2); S(2)−Ni−Cl(1) 94.33(2); S(3)−Ni−Cl(1) 95.74(2); P(1)−Ni−Cl(1) 178.21(3); P(1)−Ni−S(1) 87.58(2); P(1)−Ni−S(2) 87.39(2); P(1)−Ni−S(3) 84.19(2).

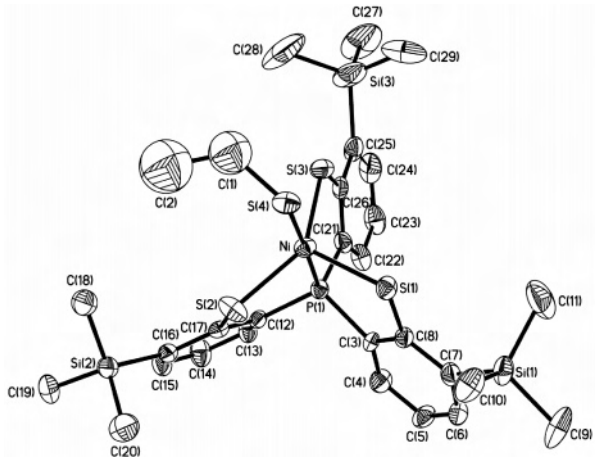

Figure 8. ORTEP drawing and labeling scheme of [Ni^{III}(SC$_2$H$_5$)(P(C$_6$H$_3$-3-SiMe$_3$-2-S)$_3$)]$^-$ (**4**) anion with thermal ellipsoids drawn at 50% probability. Selected bond distances (Å) and angles (deg): Ni−S(1) 2.2791(12); Ni−S(2) 2.2639(13); Ni−S(3) 2.2169(13); Ni−S(4) 2.2734(12); Ni−P(1) 2.1345(12); C(1)−S(4) 1.760(9); C(1)−C(2) 1.524(10); S(1)−Ni−S(2) 109.65(5); S(1)−Ni−S(3) 111.26(5); S(2)−Ni−S(3) 137.95(6); S(1)−Ni−S(4) 92.88(5); S(2)−Ni−S(4) 93.13(5); S(3)−Ni−S(4) 94.16(5); P(1)−Ni−S(4) 177.78(5); P(1)−Ni−S(1) 87.30(5); P(1)−Ni−S(2) 84.73(5); P(1)−Ni−S(3) 87.84(5); Ni−S(4)−C(1) 109.1(6).

Conclusion and Comments

Studies on the mononuclear Ni(III)−thiolate complexes (**2**−**5**, **7**, **9**) have led to the following results related to the structure, reactivity, and spectroscopic properties of the nickel center of bimetallic Ni−Fe active site of the oxidized-state [NiFe] hydrogenase.

(1) The mononuclear Ni(III)−thiolate complex **2** is more stable thermally than the corresponding Ni(III) complex [Ni^{III}(SePh)(P(*o*-C$_6$H$_4$S)$_3$)]$^-$. This result may be rationalized by the distinct electronic effects between [P(C$_6$H$_3$-3-SiMe$_3$-2-S)$_3$]$^{3-}$ and [P(*o*-C$_6$H$_4$S)$_3$)]$^{3-}$ ligands. In brief, the SiMe$_3$ group, a strongly σ-donating group, serves as an effective promoter of Ni(III) metal π-donating ability to stabilize the Ni(III)−thiolate complexes.[15a] As reflected in the shift of the half-wave potentials ($E_{1/2}$), the cyclic voltammograms of complexes [Ni^{III}(SePh)(P(*o*-C$_6$H$_4$S)$_3$)]$^-$, **2**, **4**, and **7** display reversible Ni$^{III/II}$ process with $E_{1/2}$ = −1.20, −1.26, −1.32, and −1.34 V (vs Cp$_2$Fe/Cp$_2$Fe$^+$), respectively. However, the cyclic voltammogram of complex **3** with a coordinated chloride ligand displays an irreversible reduction at −1.17 V (vs Cp$_2$Fe/Cp$_2$Fe$^+$).

(2) The thermally stable complex **4** with a monodentate ethylthiolate coordinated to the Ni(III) was isolated. The single-crystal X-ray structure shows a Ni^{III}−S(4) (ethylthiolate) bond length of 2.273(1) Å in complex **4** is in the range of 2.12−2.28 Å for the Ni^{III}−S bond lengths of the oxidized *D. gigas* hydrogenases.[2]

(3) In contrast to the inertness of complexes **3**, **7**, and **9** under a CO atmosphere, carbon monoxide did trigger the reductive elimination of the monodentate chalcogenolate ligand of complexes **2**, **4**, and **5** to yield Ni^{II}−CO complex **6** accompanied by the formation of diphenyl/dialkyl dichalcogenides. This result may provide some clues to the transformation mechanism between the Ni−L form and Ni−CO form of [NiFe] hydrogenase isolated from *D. vulgaris* Miyazaki F and CO acting as an inhibitor for catalytic activity of [NiFe] hydrogenases.[3c,d]

It is anticipated that the Ni(III)−alkylthiolate complexes containing an optimum electronic condition around Ni center may trigger heterolytic H_2 cleavage via the cooperation of Ni(III) and [SR]$^-$. However, no heterolytic H_2 cleavage reaction was observed in the THF solution of complex **4** under an atmosphere of hydrogen. The synthesis of oxygen-containing Ni(III)−thiolate complexes is ongoing.

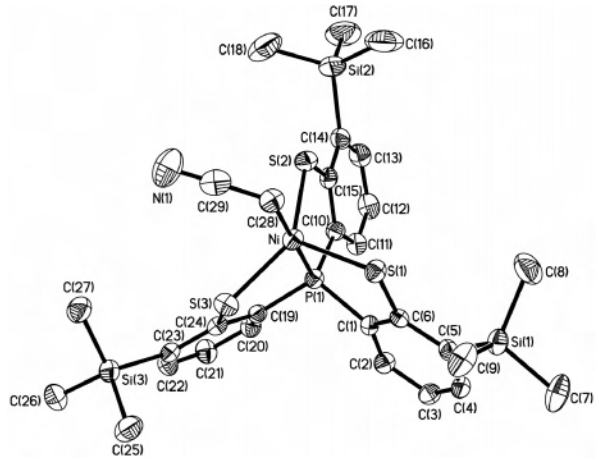

Figure 9. ORTEP drawing and labeling scheme of [Ni^{III}(CH$_2$CN)(P(C$_6$H$_3$-3-SiMe$_3$-2-S)$_3$)]$^-$ (**7**) anion with thermal ellipsoids drawn at 50% probability. Selected bond distances (Å) and angles (deg): Ni−S(1) 2.2795(8); Ni−S(2) 2.2259(9); Ni−S(3) 2.2580(9); Ni−P(1) 2.1362(8); Ni−C(28) 2.037-(3); C(28)−C(29) 1.390(5); N(1)−C(29) 1.167(4); S(1)−Ni−S(2) 109.92(3); S(1)−Ni−S(3) 110.66(3); S(2)−Ni−S(3) 138.45(3); P(1)−Ni−S(1) 87.18-(3); P(1)−Ni−S(2) 88.00(3); P(1)−Ni−S(3) 85.40(3); Ni−C(28)−C(29) 114.6(2); C(28)−Ni−P(1) 179.03(9); C(28)−Ni−S(2) 92.78(9); C(28)−Ni−S(3) 94.39(9); C(28)−Ni−S(1) 92.01(9).

(21) Holm, R. H.; Carrie, M.; Muetterties, M. C.; Stavropoulos, P. *J. Am. Chem. Soc.* **1991**, *113*, 8485−8492.
(22) Hillhouse, G. L.; Matsunaga, P. T. *J. Am. Chem. Soc.* **1993**, *115*, 2075−2077.
(23) Nelkenbaum, E; Kapon, M.; Eisen, M. S. *Organometallics* **2005**, *24*, 2645−2659.

Experimental Section

Manipulations, reactions, and transfers were conducted under nitrogen according to Schlenk techniques or in a glovebox (argon gas). Solvents were distilled under nitrogen from appropriate drying agents (diethyl ether from CaH_2; acetonitrile from $CaH_2-P_2O_5$; methylene chloride from CaH_2; hexane and tetrahydrofuran (THF) from sodium benzophenone) and stored in dried, N_2-filled flasks over 4 Å molecular sieves. Nitrogen was purged through these solvents before use. Solvent was transferred to the reaction vessel via stainless cannula under positive pressure of N_2. The reagents bis(triphenylphosphoranylidene)ammonium chloride ([PPN][Cl]) (Fluka), diphenyl diselenide, sodium ethylthiolate, di(2-thienyl) disulfide, (triphenylphosphine) nickel(II) dichloride, and deuterium oxide, 99.9 atom % D (Aldrich) were used as received. Compound tris(2-thiophenyl)phosphine ($P(C_6H_3\text{-}3\text{-}SiMe_3\text{-}2\text{-}SH)_3$) was synthesized by published procedures.[24] Infrared spectra of the ν(SH) stretching frequencies were recorded on a Perkin-Elmer model spectrum One B spectrophotometer with KBr solid. UV−vis spectra were recorded on a GBC Cintra 10e and Jusco V-570. ^{1}H and ^{2}H NMR spectra were obtained on a Varian Unity-500 spectrometer. Electrochemical measurements were performed with CHI model 421 potentionstat (CH Instrument) instrumentation. Cyclic voltammograms were obtained from 2.0 mM analyte concentration in O_2-free CH_3CN using 0.1 M [n-Bu_4N][PF_6] as a supporting electrolyte. Potentials were measured at 298 K vs a Ag/AgCl reference electrode by using a glassy carbon working electrode. Analyses of carbon, hydrogen, and nitrogen were obtained with a CHN analyzer (Heraeus).

Preparation of [PPN][Ni(SePh)(P(C_6H_3-3-$SiMe_3$-2-S)$_2$(C_6H_3-3-$SiMe_3$-2-SH))] (1). Complexes [PPN][Ni(CO)($SePh)_3$] (0.2 mmol, 0.218 g) and $P(C_6H_3\text{-}3\text{-}SiMe_3\text{-}2\text{-}SH)_3$ (0.2 mmol, 0.115 g) were loaded into a 50-mL flask and 15 mL of THF was added by cannula. The reaction mixture was stirred at ambient temperature for 1 h, and then hexane (20 mL) was added to precipitate the red-brown solid [PPN][Ni(SePh)(P(C_6H_3-3-$SiMe_3$-2-S)$_2$(C_6H_3-3-$SiMe_3$-2-SH))] (**1**) (yield 0.225 g, 85%).[14] Diffusion of diethyl ether into THF solution of complex **1** at room temperature for 1 week yielded layered brown-red crystals of complex **1** (yield 0.212 g, 80%). IR: 2250 w (ν_{SH}) cm^{-1} (KBr).[14] ^{1}H NMR (C_4D_8O): δ 8.59 (d) (SH), 6.65−6.77 (m), 6.87 (t), 7.15−7.33 (m) (PhSe, P(C_6H_3-3-$SiMe_3$-2-S)$_3$); 0.20 (s), 0.30 (s) ($SiMe_3$) ppm. Absorption spectrum (THF) [λ_{max}, nm (ϵ, M^{-1} cm^{-1})]: 420 (2700), 500 (1150). Anal. Calcd for $C_{69}H_{72}NNiP_3S_3SeSi_3$: C, 62.48; H, 5.47; N, 1.06. Found: C, 62.18; H, 5.12; N, 0.98.

D/H Exchange for Reaction of Complex 1 and D_2O. To a THF (10 mL) solution of complex **1** (0.133 g, 0.1 mmol) at 5 °C, a 100-fold excess of D_2O (0.18 mL, 10 mmol) was added. The reaction solution containing the mixture solution of complex **1** and D_2O was stirred for 24 h at 5 °C. Hexane (15 mL) was then added slowly to layer above the mixture solution. The flask was tightly sealed and kept at room temperature for 1 week. Red-brown crystals [PPN][Ni(SePh)(P(C_6H_3-3- $SiMe_3$-2-S)$_2$(C_6H_3-3-$SiMe_3$-2-SD))] (**1-D**) were isolated (0.08 g, 60%). IR (KBr): 1665 (ν_{SD}) cm^{-1}. ^{2}H NMR (C_4H_8O): δ 8.43 (br) ppm (SD) vs C_4H_8O (natural abundance of D in C_4H_8O solvent, δ 1.73 and 3.58 ppm).

Preparation of [PPN][Ni(SePh)(P(C_6H_3-3-$SiMe_3$-2-S)$_3$)] (2). Pure oxygen gas (0.62 mL) was injected through a red-brown THF solution (10 mL) of complex **1** (0.133 g, 0.1 mmol) at room temperature. The resulting deep-green solution was reduced in volume under vacuum, and diethyl ether was then added to precipitate the dark-green solid [PPN][Ni(SePh)(P(C_6H_3-3-$SiMe_3$-2-S)$_3$)] (**2**) (0.118 g, 90%). Diffusion of diethyl ether into a THF−MeCN (3:1 volume ratio) solution of complex **2** at −15 °C for 4 weeks yielded dark-green crystals suitable for X-ray crystallography. ^{1}H NMR (CD_3CN): δ −4.25 (br), 3.03 (br), 6.50 (br), 10.15 (br), 11.01 (br), 14.77 (br) (SePh, o-C_6H_3S); 2.13 (s), 2.24 (s) ($SiMe_3$) ppm. Absorption spectrum (CH_3CN) [λ_{max}, nm (ϵ, M^{-1} cm^{-1})]: 304 (21000), 356 (13000), 590 (2500), 771 (800), 954 (970). Anal. Calcd for $C_{69}H_{71}NP_3Si_3S_3SeNi$: C, 62.53; H, 5.40; N, 1.06. Found: C, 62.41; H, 5.10; N, 0.81.

Preparation of [PPN][Ni(Cl)(P(C_6H_3-3-$SiMe_3$-2-S)$_3$)] (3). A portion 15 mL of CH_2Cl_2 was added into a 50-mL flask loaded with complex **2** (0.132 g, 0.1 mmol), and the reaction mixture was allowed to stir at ambient temperature for 48 h. A change in color from dark green to light green occurred, and 20 mL of hexane was then added to precipitate the green solid complex [PPN][Ni(Cl)-(P(C_6H_3-3-$SiMe_3$-2-S)$_3$)] (**3**) (0.102 g, 85%). Diffusion of hexane into a CH_2Cl_2 solution of complex **3** at room temperature for 1 week led to dark-green crystals suitable for X-ray crystallography. ^{1}H NMR (CD_3CN): δ −6.47 (br), 9.59 (br), 16.20 (br) (o-C_6H_3S); 2.12 (s), 2.31 (s) ($SiMe_3$) ppm. Absorption spectrum (CH_3CN) [λ_{max}, nm (ϵ, M^{-1} cm^{-1})]: 430 (6000), 620 (2200), 760 (1650), 990 (1000). Anal. Calcd for $C_{63}H_{66}NP_3Si_3S_3ClNi$: C, 62.81; H, 5.52; N, 1.16. Found: C, 62.24; H, 5.03; N, 1.49.

Preparation of [PPN][Ni(SC_2H_5)(P(C_6H_3-3-$SiMe_3$-2-S)$_3$)] (4). A CH_3CN−THF solution (5:15 mL) of complex **3** (0.242 g, 0.2 mmol) was added to a CH_3CN solution of [Na][SC_2H_5] (0.034 g, 0.4 mmol) by cannula under positive N_2. The resulting mixture was stirred at room temperature for 2 h and then filtered through Celite to remove [Na][Cl]. Diethyl ether (20 mL) was added to precipitate the dark green solid [PPN][Ni(SC_2H_5)(P(C_6H_3-3-$SiMe_3$-2-S)$_3$)] (**4**) (0.147 g, 60%) after the solution was concentrated to 8 mL. Diffusion of diethyl ether into CH_3CN−THF solution of complex **4** at −15 °C for 4 weeks led to dark green crystals suitable for X-ray crystallography. ^{1}H NMR (CD_3CN): δ 40.67 (br), 3.17 (br) (SEt); −3.05 (br), 10.27 (br), 14.97 (br) (o-C_6H_3S); 2.10 (s), 2.34 (s) ($SiMe_3$) ppm. Absorption spectrum (CH_3CN) [λ_{max}, nm (ϵ, M^{-1} cm^{-1})]: 360 (11285), 500 (1760), 579 (2435), 724 (885), 922 (960), 1123(615). Anal. Calcd for $C_{65}H_{66}NP_3Si_3S_4Ni$: C, 63.71; H, 5.43; N, 1.14. Found: C, 63.71; H, 5.51; N, 1.34.

Preparation of [PPN][Ni^{III}(2-S−C_4H_3S)(P(C_6H_3-3-$SiMe_3$-2-S)$_3$)] (5). Method (a): A THF−CH_3CN solution (10:5 mL) of complex **3** (0.242 g, 0.2 mmol) was added to a CH_3CN solution of [Na][2-S−C_4H_3S] (0.028 g, 0.2 mmol). The resulting mixture was stirred at room temperature for 3 h and then filtered through Celite to remove [Na][Cl]. Diethyl ether (20 mL) was added to precipitate the green solid [PPN][Ni^{III}(2-S−C_4H_3S)(P(C_6H_3-3-$SiMe_3$-2-S)$_3$)] (**5**) (yield 0.154 g, 60%). Method (b): Di(2-thienyl) disulfide (0.23 g, 1 mmol) and [PPN][$HFe(CO)_4$] (0.283 g, 0.4 mmol) were loaded into a 20-mL Schlenk tube and dissolved in THF (5 mL). After the reaction solution was stirred for 15 min at ambient temperature, the solution was transferred to another Schlenk flask containing $[NiCp(CO)]_2$ (0.061 g, 0.2 mmol) by cannula under a positive pressure of N_2. The reaction mixture was stirred for 6 h at ambient temperature, and hexane (10 mL) was added to precipitate the brown oily product [PPN][Ni(CO)(2-S−$C_4H_3S)_3$].[15c,d] The brown oily product was dried under N_2 purge and redissolved in THF. The THF solution of [PPN][Ni(CO)(2-S−$C_4H_3S)_3$] was then transferred to another Schlenk flask containing $P(C_6H_3\text{-}3\text{-}SiMe_3\text{-}2\text{-}SH)_3$ (0.23 g, 0.4 mmol) by cannula under positive N_2. After the reaction mixture was stirred for 30 min under N_2, degassed hexane (25 mL) was added to precipitate the red-brown solid [PPN][Ni^{II}(2-S−C_4H_3S)(P(C_6H_3-3-$SiMe_3$-2-S)$_2$(C_6H_3-3-$SiMe_3$-2-SH))] (yield 0.324

(24) Block, E.; Ofori-Okai, G; Zubieta, J. *J. Am. Chem. Soc.* **1989**, *111*, 2327−2329.

g, 63%) characterized by EA (Anal. Calcd for $C_{67}H_{70}NP_3Si_3S_5Ni$: C, 62.60; H, 5.49; N, 1.09. Found: C, 62.43; H, 5.56; N, 0.94), IR, and single-crystal X-ray diffraction.[14a] Pure oxygen gas (10 mL) was injected into the red-brown THF solution (20 mL) of complex [Ni^{II}(2-S−C$_4$H$_3$S)(P(C$_6$H$_3$-3-SiMe$_3$-2-S)$_2$(C$_6$H$_3$-3-SiMe$_3$-2-SH))]$^-$ and stirred for 1 h at room temperature. The resulting green solution was reduced in volume under vacuum, and then hexane was added to precipitate the green solid [PPN][Ni^{III}(2-S−C$_4$H$_3$S)(P(C$_6$H$_3$-3-SiMe$_3$-2-S)$_3$)] (**5**). Diffusion of hexane into a THF solution of complex **5** at 4 °C for 1 week led to green crystals suitable for X-ray crystallography (Supporting Information Figure S5). ^{1}H NMR (CD$_3$CN): δ −6.44 (br), 9.58 (br), 16.20 (br) (*o*-C$_6$H$_3$S); 0.37 (s), 0.60 (s) (SiMe$_3$) ppm. Absorption spectrum (THF) [λ_{max}, nm (ϵ, M^{-1} cm^{-1})]: 372 (2336), 435 (1612), 598 (686), 973 (242). Anal. Calcd for $C_{67}H_{69}NP_3Si_3S_5Ni$: C, 62.60; H, 5.41; N, 1.09. Found: C, 62.39; H, 5.10; N, 0.88.

Reaction of Complex 2 (or 4 and 5) and CO. The 50-mL flask containing a THF−CH$_3$CN solution (10:5 mL, v/v) of complex **2** (0.067 g, 0.05 mmol) (or complex **4**/**5** (0.05 mmol)) was filled with pure CO gas (28 psi, at 293 K) and tightly sealed. After the reaction solution was stirred at ambient temperature for 1 week, the color of solution gradually turned from dark green to light green accompanied by trace of white solid precipitate. The resulting mixture was filtered and solvent was removed from the filtrate under vacuum to leave the dark green solid. Hexane (10 mL) was added to extract the (PhSe)$_2$ (0.007 g, 80%) identified by EI-MS and the left dark green solid [PPN][Ni(CO)(P(C$_6$H$_3$-3-SiMe$_3$-2-S)$_3$)] (**6**) characterized by IR, UV−vis, and single-crystal X-ray diffraction. Diffusion of diethyl ether into a THF−CH$_3$CN (2:1 v/v) of complex **6** at room temperature for 1 week led to dark green crystals suitable for X-ray crystallography (0.036 g, 60%).[10e] IR (ν_{CO}): 2033 vs (CH$_3$CN), 2033 vs cm^{-1} (KBr). ^{1}H NMR (CD$_2$Cl$_2$): δ 6.77 (td), 7.10 (td), 7.23 (dd), (P(C$_6$H$_3$-3-SiMe$_3$-2-S)$_3$); 0.06 (s), 0.35 (s) (SiMe$_3$) ppm. Absorption spectrum (CH$_3$CN) [λ_{max}, nm (ϵ, M^{-1} cm^{-1})]: 711 (1350). Anal. Calcd for $C_{64}H_{61}NOP_3Si_3S_3Ni$: C, 64.47; H, 5.16; N, 1.17. Found: C, 65.07; H, 4.33; N, 1.26.

Preparation of [PPN][Ni(CH$_2$CN)(P(C$_6$H$_3$-3-SiMe$_3$-2-S)$_3$)] (7). A portion of CH$_3$CN (15 mL) was added into a 50-mL flask loaded with complex **3** (0.242 g, 0.2 mmol) and NaH (0.015 g, ∼0.6 mmol). The resulting mixture was stirred at ambient temperature for 1 h and then filtered through Celite to remove [Na][Cl]. The purple solution was concentrated under vacuum, and diethyl ether was added to precipitate the dark purple solid [PPN][Ni(CH$_2$CN)(P(C$_6$H$_3$-3-SiMe$_3$-2-S)$_3$)] (**7**) (0.167 g, 65%). Diffusion of diethyl ether into CH$_3$CN solution of complex **7** at −15 °C for 4 weeks led to dark purple crystals suitable for X-ray crystallography. IR: 2192 m (ν_{CN}) cm^{-1} (KBr, CH$_3$CN). ^{1}H NMR (CD$_3$CN): δ 84.50 (br) (−CH$_2$CN); −4.71 (br), 12.10 (br), 14.30 (br) (*o*-C$_6$H$_3$S); 2.17 (s) (SiMe$_3$) ppm. Absorption spectrum (CH$_3$CN) [λ_{max}, nm (ϵ, M^{-1} cm^{-1})]: 356 (12720), 543 (3490), 648 (1500), 925 (1700). Anal. Calcd for $C_{65}H_{68}N_2P_3Si_3S_3Ni$: C, 64.56; H, 5.67; N, 2.32. Found: C, 64.69; H, 5.55; N, 2.09.

Preparation of [Ni^{II}(PPh$_3$)(P(C$_6$H$_3$-3-SiMe$_3$-2-S)$_2$(C$_6$H$_3$-3-SiMe$_3$-2-SH))] (8). NiCl$_2$(PPh$_3$)$_2$ (0.131 g, 0.2 mmol) and P(C$_6$H$_3$-3-SiMe$_3$-2-SH)$_3$ (0.115 g, 0.2 mmol) were dissolved in THF (10 mL) and stirred under N$_2$ atmosphere for 30 min at ambient temperature. Hexane (20 mL) was then added to precipitate the brown solid [PPN][Ni^{II}(PPh$_3$)(P(C$_6$H$_3$-3-SiMe$_3$-2-S)$_2$(C$_6$H$_3$-3-SiMe$_3$-2-SH))] (**8**) (yield 0.114 g, 64%). Diffusion of hexane into the THF solution of complex **8** at room temperature for 4 days led to red-brown crystals suitable for X-ray crystallography (Supporting Information Figure S10). ^{1}H NMR (CD$_3$Cl): δ 0.11 (s) (SiMe$_3$); 6.26 (s) (SH); 6.92 (br), 7.2 (br), 7.4 (br), 7.68 (br) (PPh$_3$, *o*-C$_6$H$_3$S) ppm. IR (KBr): 2192 (ν_{SH}) cm^{-1}.[14] Absorption spectrum (THF) [λ_{max}, nm (ϵ, M^{-1} cm^{-1})]: 385 (1221), 623 (245). Anal. Calcd for $C_{45}H_{52}P_2Si_3S_3Ni$: C, 60.46; H, 5.86. Found: C, 59.84; H, 5.66.

Preparation of [Ni^{III}(PPh$_3$)(P(C$_6$H$_3$-3-SiMe$_3$-2-S)$_3$)] (9). Dry oxygen gas (2.48 mL) was purged through a red THF solution (10 mL) of complex **8** (0.388 g, 0.4 mmol) at room temperature. The reaction solution was stirred for 1 h and a significant change in color of the reaction solution from red to deep green was observed. After the solution was concentrated to 5 mL, hexane (15 mL) was then added to precipitate the dark green solid [Ni^{III}(PPh$_3$)(P(C$_6$H$_3$-3-SiMe$_3$-2-S)$_3$)] (**9**) (yield 0.207 g, 58%).[14b] Diffusion of hexane into a THF solution of complex **9** at 0 °C for 3 weeks led to dark green crystals. ^{1}H NMR (CD$_3$Cl): δ −10.71 (br), 11.29 (br), 15.85 (br) (*o*-C$_6$H$_3$S); 7.24 (br), 7.76 (br) (PPh$_3$); 2.76 (s) (SiMe$_3$) ppm. Absorption spectrum (THF) [λ_{max}, nm (ϵ, M^{-1} cm^{-1})]: 381 (4770), 620 (1700), 682 (1620), 1167 (1000). Anal. Calcd for $C_{45}H_{51}P_2Si_3S_3Ni$: C, 60.53; H, 5.76. Found: C, 59.95; H, 5.26.

Kinetic Measurements. The reaction between complex **2** (or **4**) and CH$_2$Cl$_2$ was followed by UV−vis with the intensity increase of the characteristic absorption at 760 nm due to the formation of complex **3** at 23 (±1) °C. Complex **2** (0.0014 g, 0.001 mmol) was loaded into a 4-mL UV Precision cell (Hellma, 10.00-mm light path) and then CH$_2$Cl$_2$ (4.0 mL) was injected to dissolve it. The reaction was monitored by UV−vis using time scan model with the integration time (2 s) and the internal time (10 min) for 20 h. This reaction obeyed pseudo-first-order kinetics in the presence of an excess amount of CH$_2$Cl$_2$ over 20 h, and the rate constant (k_{obs} = (4.78 ± 0.02) × 10^{-5} s^{-1}) (R^2 = 0.9990) was determined by fits of data using the Sigmaplot2001 software. The kinetics of the reaction of complex **4** (0.0012 g, 0.001 mmol) and CH$_2$Cl$_2$ (4.0 mL) were monitored by UV−vis spectrometer using time scan model with the following parameters: the integration time (2 s), the internal time (1 min), and reaction time (2 h). This reaction also obeyed pseudo-first-order kinetics with the rate constant (k_{obs} = (6.01 ± 0.03) × 10^{-4} s^{-1}) (R^2 = 0.9990).

EPR Measurements. EPR measurements were performed at X-band using a Bruker EMX spectrometer equipped with a Bruker TE102 cavity and a Bruker VT2000 temperature control unit (120−300 K). The microwave frequency was measured with a Hewlett-Packard 5246L electronic counter. X-band EPR spectra of complexes **2**−**4** in CH$_3$CN were obtained with a microwave power of 20.0, 20.3, and 19.9 mW, frequency at 9.602, 9.602, and 9.606 GHz, and modulation amplitude of 1.6, 1.6, and 0.4 G at 100 kHz, respectively.

Magnetic Measurements. The magnetization data were recorded on a SQUID magnetometer (MPMS5 Quantum Design company) with an external 0.5 T magnetic field for complexes **2** and **3** in the temperature range 2−300 K. The magnetic susceptibility of the experimental data was corrected for diamagnetism by the tabulated Pascal's constants.

Crystallography. The crystals chosen for X-ray diffraction studies measured 0.32 × 0.21 × 0.20 mm for complex **2**, 0.40 × 0.30 × 0.20 mm for complex **3**, 0.40 × 0.35 × 0.25 mm for complex **4**, and 0.45 × 0.35 × 0.15 mm for complex **7**, respectively. Each crystal was mounted on a glass fiber and quickly coated in epoxy resin. Unit-cell parameters were obtained by least-squares refinement. Diffraction measurements for complexes **2**, **3**, **4**, and **7** were carried out on a SMART CCD (Nonius Kappa CCD) diffractometer with graphite-monochromated Mo Kα radiation (λ = 0.7107 Å) and between 1.41 and 27.50° for complex **2**, between

1.42 and 27.50° for complex **3**, between 1.45 and 27.50° for complex **4**, and between 1.64 and 27.50° for complex **7**. Least-squares refinement of the positional and anisotropic thermal parameters of all non-hydrogen atoms and fixed hydrogen atoms was based on F^2. A SADABS absorption correction was made.[25] The SHELXTL structure refinement program was employed.[26]

(25) Sheldrick, G. M. *SADABS, Siemens Area Detector Absorption Correction Program*; University of Göttingen: Germany, 1996.
(26) Sheldrick, G. M. *SHELXTL, Program for Crystal Structure Determination;* Siemens Analytical X-ray Instruments Inc.: Madison, WI, 1994.

Acknowledgment. We gratefully acknowledge financial support from the National Science Council of Taiwan.

Supporting Information Available: X-ray crystallographic files in CIF format for the structural determinations of complexes **2**−**8**, crystallographic data and refinement parameters, and bond distances and angles. This material is available free of charge via the Internet at http://pubs.acs.org.

IC061399G